Elrayess, M., Almuraikhy, S., Kafienah, W., Al-Menhali, A., Al-Khalaifi, F., Bashah, M., ... Jaganjac, M. (2017). 4-hydroxynonenal causes impairment of human subcutaneous adipogenesis and induction of adipocyte insulin resistance. *Free Radical Biology and Medicine*, *104*, 129–137. https://doi.org/10.1016/j.freeradbiomed.2017.01.015

Title: 4-hydroxynonenal causes impairment of human subcutaneous adipogenesis and induction of adipocyte insulin resistance

Mohamed Elrayess[a,+], Shamma Al-Muraikhy[a,b,+], Wael Kafienah[b], Afnan Al-Menhali[a], Fatima Al-Khalaifi[a], Moataz Bashah[c], Kamelija Zarkovic[d], Neven Zarkovic[e], Georg Waeg[f], Mohammed Alsayrafi[a], Morana Jaganjac[a,*]

a Anti Doping Lab Qatar, Sports City, Doha, Qatar.

b School of Cellular and Molecular Medicine, University of Bristol, Bristol, United Kingdom.

c Bariatric and Metabolic Surgery, Hamad Medical Corporation, Doha, Qatar.

d Department of Pathology, Medical Faculty University of Zagreb, Clinical Hospital Centre Zagreb, Zagreb, Croatia

e Laboratory for Oxidative Stress, Department of Molecular Medicine, Rudjer Boskovic Institute, Zagreb, Croatia

f Institute of Molecular Biosciences, University of Graz, Graz, Austria

[+] Both authors contributed equally to this work

***Corresponding author:**

Morana Jaganjac,

Toxicology and multipurpose division,

ADLQ, P.O.Box 27775,

Doha, Qatar

Office: (974) 4413 2846

Mobile: (974) 5509 2537

Fax: (974) 44132997

E-mail: mjaganjac@adlqatar.qa

Abbreviations:

2',7'-dichlorfluorescein-diacetate (DCFH-DA); 4′,6-Diamidino-2-phenylindole dihydrochloride (DAPI); alanine transaminase (ALT); alkaline phosphatase (ALP); aspartate aminotransferase (AST); diastolic blood pressure (DBP); 2',7'-dichlorfluorescein-diacetate (DCFH-DA); 4′,6-Diamidino-2-phenylindole dihydrochloride (DAPI); fasting plasma glucose (FPG); fatty acid synthase (FASN); Fatty acid-binding protein 4 (FABP4); Haematoxylin/Eosin (HE); Hamad Medical Corporation (HMC); high density lipoprotein (HDL); 4-hydroxynonenal (4-HNE);

homeostatic model assessment (HOMA-IR); immunohistochemical (IHC); insulin sensitive (IS); insulin resistant (IR); low density lipoprotein (LDL); mean arterial blood pressure (MAP); metabolically healthy obese (MHO); peroxiredoxin 2 (PRX2); polyunsaturated fatty acids (PUFAs); reactive oxygen species (ROS); relative fluorescence units (RFU); sterol regulatory element binding transcription factor 1 (SREBF1); Stromal-vascular fraction (SVF); subcutaneous (SC); superoxide dismutase 1 (SOD1); superoxide dismutase 2 (SOD2); systolic blood pressure (SBP); thioredoxin (TRX1)

Funding: This work was supported by Qatar National Research Fund [QNRF grant number NPRP6-235-1-048].

Abstract

Objective. Increased adipose production of 4-hydroxynonenal (4-HNE), a bioreactive aldehyde, directly correlates with obesity and insulin resistance. The aim of this study was to elucidate the impact of 4-HNE in mediating adipocyte differentiation and function in two metabolically distinct obese groups; the insulin sensitive (IS) and the insulin resistant (IR).

Methods. Subcutaneous (SC) adipose tissues were obtained from eighteen clinically well characterized obese premenopausal women undergoing weight reduction surgery. Cellular distribution of 4-HNE in the form of protein adducts was determined by immunohistochemistry in addition to its effect on oxidative stress, cell growth, adipogenic capacity and insulin signaling in preadipocytes derived from the IS and IR participants.

Results. 4-HNE was detected in the SC adipose tissue in different cell types with the highest level detected in adipocytes and blood vessels. Short and long-term *in vitro* treatment of SC preadipocytes with 4-HNE caused inhibition of their growth and increased production of reactive oxygen species (ROS) and antioxidant enzymes. Repeated 4-HNE treatment led to a greater reduction in the adipogenic capacity of preadipocytes from IS subjects compared to IR and caused dephosphorylation of IRS-1 and p70S6K while activating GSK3α/β and BAD, triggering an IR phenotype.

Conclusion. These data suggest that 4-HNE-induced oxidative stress plays a role in the regulation of preadipocyte growth, differentiation and insulin signaling and may therefore contribute to adipose tissue metabolic dysfunction associated with insulin resistance.

Keywords:

4-hydroxynonenal; adipogenesis; insulin resistance; insulin sensitivity; obesity preadipocytes; redox homeostasis; subcutaneous fat

Introduction

Obesity constitutes a major health problem in developed countries, and is increasingly becoming one in the developing world. However, a subset of obese individuals, known as the insulin sensitive (IS) obese or metabolically healthy obese (MHO), maintain insulin sensitivity and exhibit less metabolic abnormalities than their equally obese insulin resistant (IR) counterpart [1, 2]. The transient nature of the protective phenotype of IS obesity, which may shift towards a more adaptable insulin resistant (IR) obesity over time, was previously suggested [3].

Obesity causes subcutaneous (SC) fat dysfunction, leading to a reduction in the number of differentiating preadipocytes and hypertrophy of mature adipocytes, predisposing adipose tissue to insulin resistance [4-6]. Obesity-associated insulin resistance is marked by impaired SC adipogenesis while IS obese individuals exhibit a more efficient adipogenesis [7]. This contributes to the expansion of visceral fat in IR obese subjects with ectopic fat deposition in the liver, skeletal muscle and other depots such as epicardial fat [8], causing further augmentation of IR in these tissues [9].

Fat accumulation within the adipose tissue correlates with markers of systemic oxidative stress as an early mediator of metabolic syndrome [10]. Increased production of reactive oxygen species (ROS) in the adipose tissue causes lipid peroxidation and tissue dysfunction [10]. One of the ROS main targets are polyunsaturated fatty acids (PUFAs) that are esterified in the membrane or storage lipids [11]. PUFA-derived reactive aldehydes have an important role in cellular signaling, proliferation and differentiation, both under physiological as well as pathological conditions [12, 13]. 4-hydroxynonenal (4-HNE) is the most abundant lipid peroxidation product of arachidonic acid and a key mediator of oxidant-induced cell signaling and apoptosis [14]. The cellular concentration of 4-HNE varies from 0.1 to 0.3 μM under physiological conditions and from 10 μM up to 5 mM under oxidative stress [15, 16]. Differences in the redox status and increased 4-HNE levels of human adipose tissues in relation to obesity and metabolic risk were previously reported [17]. This elevation can progressively impair cell structure and

function due to the accumulation of stable adducts formed with proteins, phospholipids and DNA [18, 19]. The generation of high levels of 4-HNE has been associated with inflammatory processes [20-22] through the activation of cyclooxygenase [23], under pathological conditions such as insulin resistance, atherosclerosis and obesity [24].

Increased intracellular 4-HNE accumulation in adipose tissues contributes to obesity-related lipolytic activation [25]. The role of 4-HNE on impairment of adipocyte differentiation was shown in 3T3L1 murine preadipocytes, where short-term as well as repeated exposure of these cells to physiological concentrations of 4-HNE promoted subsequent oxidative stress, impaired adipogenesis, alteration of the expression of adipokines, increased lipolytic gene expression and free fatty acids release [26]. These effects were suggested more recently to be mediated by a decrease in aldehyde dehydrogenase 2 activity [27].

In the present study, we hypothesize that *in vitro* long-term exposure of SC preadipocytes from IS individuals to 4-HNE can impair their adipogenesis and insulin sensitivity, rendering their behavior like that seen in preadipocytes from IR individuals.

Materials and methods

Materials

IL-6 and leptin ELISAs were purchased from R&D systems (UK) and Insulin ELISA from Mercodia Diagnostics (Sweden). 3,3' Diaminobenzidine tetrahydrochloride and LSAB kit were obtained from DAKO (Denmark). OxiSelect hydrogen peroxide/peroxidase assay kit was obtained from Cell Biolabs (UK). DAPI and LipidTOX™ Green Neutral Lipid were purchased from Life Technologies (UK). Nitrocellulose membranes were obtained from Amersham (UK). Secondary antibody solution EnVision and 3,30-diaminobenzidine tetra-hydrochloride were purchased from Dako (Denmark). Human 4-HNE ELISA kit (CSB-E16214h) was purchased from Cusabio (China). RNAeasy extraction kit, first strand cDNA synthesis kit and RT2 Profiler human insulin resistance PCR arrays were from Qiagen (UK). Milliplex(r) Map Human Panel Oxidative stress Magnetic Bead Panel (H0XSTMAG-18K) was purchased from Millipore (UK) and Bio-Plex Pro™ Cell Signaling Akt Panel, 8-plex (LQ00006JK0K0RR) from Bio-Rad (UK). Other chemicals and reagents were purchased from Sigma (Germany) unless indicated otherwise.

Cohort

Eighteen obese and morbidly obese premenopausal females were recruited among patients undergoing weight reduction surgery at Hamad Medical Corporation (HMC) in Doha, Qatar. All participants provided informed consents before surgery. All protocols were approved by the Institutional Research Boards of ADLQ and HMC (SCH-ADL-070, SCH-JOINT-111). Anthropometric and plasma measures were determined as described previously [7], including systolic (SBP), diastolic blood pressure (DBP), mean arterial blood pressure (MAP), low density lipoprotein (LDL), high density lipoprotein (HDL), total cholesterol, triglycerides, fasting plasma glucose (FPG), IL-6, Leptin, insulin, alkaline phosphatase (ALP), aspartate aminotransferase (AST), alanine transaminase (ALT), bilirubin, and total protein. Insulin resistance was calculated by the homeostatic model assessment (HOMA-IR) [28] using 2.4 as a cutoff point (30th percentile). Accordingly, subjects were dichotomized into IS (HOMA-IR < 2.4, 9

subjects) and non-diabetic IR (HOMA-IR > 2.4, 9 subjects). SC adipose tissues of 1 to 5 g biopsies were collected from all participating subjects during their surgeries and were immediately transported to laboratory for processing.

Immunohistochemical analysis of 4-HNE

Ten adipose tissue samples were randomly selected for immunohistochemical analysis. Adipose tissue biopsies were formalin-fixed and paraffin-embedded. Sections made from paraffin blocks were stained with Hematoxylin/Eosin (HE). 4-HNE staining was performed using our genuine monoclonal antibody specific for HNE-histidine [29, 30]. Monoclonal antibody was obtained from the culture medium of the clone derived from a fusion of Sp2-Ag8 myeloma cells with B-cells of a BALBc mouse immunized with HNE modified keyhole limpet hemocyanine [29]. The clone 1g4h7 TC antibody is specific for the HNE-histidine epitope in HNE-protein (peptide) conjugates. The dot-blot immunochemistry was used to verify the efficiency of monoclonal antibody used for detection of 4-HNE- His adducts by immunohistochemistry. Briefly, the 5% solution of BSA containing final concentrations of 4-HNE ranging from 1 to 100 µM were used for comparison to the control BSA solution without 4-HNE. Two hundred microliters of thus prepared solutions were spotted onto nitrocellulose membranes. Each membrane was incubated in blocking solution (2% non-fat milk powder in phosphate buffer) at room temperature for 60 min and subsequently incubated overnight with mouse monoclonal antibodies against 4-HNE-His adducts. The membranes were afterwards washed and incubated for 30 min with the secondary antibody solution EnVision diluted 1:25 in PBS. Immune complexes were visualized using 3,30-diaminobenzidine tetra-hydrochloride staining.

For the immunohistochemical detection of the HNE-protein adducts the immunoperoxidase technique was used using EnVision kit (Dako, Denmark) as described previously [31]. Briefly, first step included 2 hours incubation with monoclonal anti-HNE antibody (dilution 1:10) while the other two steps were performed using EnVision kit according to manufacturers' instructions. 3,3' Diaminobenzidine tetrahydrochloride was used as a chromogen in the HE counterstained sections. Immunohistochemical investigation of HNE positivity was determined by an experienced pathologist without

prior knowledge of the experimental groups and scored in a semiquantitative way described before and often used for clinical studies [32] (- 0% positive cells, + <5% positive cells, ++ 5-25% positive cells, +++ 25-50% positive cells, ++++ >50% positive cells). The presence of HNE-protein adducts in adipocytes, connective tissues, inflammatory cells and blood vessels was defined as negative (-) in the absence of the HNE-protein adducts, or as low positive (+, ++) or high positive (+++, ++++) in the presence of the HNE-protein adducts [33].

Isolation of stromal-vascular fraction cells from human SC adipose tissues

Stromal-vascular fraction (SVF) was obtained by collagenase digestion as previously described [34]. The SVF pellet was re-suspended in stromal medium (DMEM-F12, 10% FBS, Pen/Strep) and maintained in a humidified incubator at 37 °C with 5% CO2 until confluence, then passaged at $4x10^4/cm^2$ when necessary.

4-HNE preparation

The aldehyde was obtained in the form of 4-Hydroxynonenal-dimethylacetal. Prior to the experiment it was activated with 1 mM cold HCl for 1 hour at 4°C. For the experiment HNE was diluted in DMEM-F12 medium.

Proliferation assay

Cells (passage 1-5) were grown in medium (DMEM-F12, Pen/Strep) containing 3% FBS in the absence or presence of different concentrations of 4-HNE ranging from 2.5-40μM for 4 days. Cells were then fixed with formalin for 10 min, stained with 4′,6-Diamidino-2-phenylindole dihydrochloride (DAPI) and total nuclei number quantified by ArrayScan XTI (Thermo Scientific).

Differentiation assays

Cells (passage 1-5) were either grown in differentiation medium (DMEM-F12, 3% FBS, 33 μM bioten, 17 μM d-pantothenate, 1 μM dexamethasone, 250 μM of methylisobutylxanthine, 0.1 μM human insulin, 5 μM of PPARγ agonist, rosiglitazone) in the presence or absence of 5 or 10 μM of 4-HNE for 7 days, followed by 7 days

incubation in maintenance medium containing the same components as the differentiation medium except for methylisobutylxanthine and rosiglitazone as described previously [35]. To determine differentiation capacity, cells were fixed with 4% formalin for 10 min, stained with DAPI and subsequently with HCS Lipidtox for 20 min. Total number of nuclei (DAPI) and differentiated adipocytes (Lipidtox positive cells) were scored by ArrayScan XTI (Thermo Scientific) using spot detection module. Differentiation capacity was assessed by calculating the ratio of Lipidtox positive cells/total number of stained nuclei and presented as a percentage (differentiation capacity).

Measuring endogenous 4-HNE protein adduct levels in preadipocyte cultures

Paired cultures of proliferating and differentiating preadipocytes were lysed and endogenous 4-HNE levels were measured in 85µg protein lysates using human 4-HNE ELISA according to manufacture's instructions.

Gene expression analysis of sterol regulatory element binding transcription factor 1 (SREBF1), fatty acid synthase (FASN) and Fatty acid-binding protein 4 (FABP4) in response to 4-HNE treatment

Preadipocytes were treated with 10µM 4-HNE every three days for the entire differentiation period. RNA was extracted using RNAeasy kit and cDNA was synthesized using first strand cDNA synthesis kit according to manufacturer's instructions.
RT^2 Profiler human insulin resistance PCR arrays were used to simultaneously examine the mRNA levels of 89 genes, including five "housekeeping genes" in 96-well plates according to manufacturer's protocol. Genes included Sterol Regulatory Element Binding Transcription Factor 1 (SREBF1), fatty acid synthase (FASN) and Fatty acid-binding protein 4 (FABP4). Data were normalized with the internal housekeeping genes and ΔΔCt was calculated using ΔCt from proliferating IS-SC as the control group according to manufacturer's protocol.

Adipocyte oxidative stress assay in response to 4-HNE treatment

Intracellular ROS production was evaluated using 2',7'-dichlorfluorescein-diacetate (DCFH-DA, Fluka) probe as previously described [36]. Briefly, cells were pretreated

with 10 µM DCFH-DA in the HBSS in 5% CO2 / 95% air at 37°C for 30 min followed by removal of excess probe and treatment with 5 and 10uM of 4-HNE in stromal medium with 3% FBS. The fluorescence intensity was measured continuously throughout 12 hours using TECAN Infinite M200 PRO plate reader equipped with gas control mode to maintain 37°C and 5% CO2, with an excitation wavelength of 500 nm and emission detection at 529 nm. The arbitrary units, relative fluorescence units (RFU), were based directly on fluorescence intensity. Intracellular ROS production was also evaluated using aminotriazole assay as described previously [37] using OxiSelect hydrogen peroxide/peroxidase assay kit following 12 hours of 10µM 4-HNE treatment according to manufacturer's instructions.

Cellular antioxidant defense systems analyses in response to 4-HNE treatment

The effect of 4-HNE treatment on the levels of antioxidant proteins in human preadipocytes was quantified following 1, 4 and 15 days of treatment. Briefly, preadipocytes were treated with 10µM of 4-HNE one day post-seeding for one day (baseline levels), 4 days (proliferation) or 15 days (differentiation), then lysed and assayed using a commercial human 5-plex Milliplex(r) Map Human Panel Oxidative stress Magnetic Bead Panel (H0XSTMAG-18K) kit following manufacturer's instructions. The panel included catalase, thioredoxin (TRX1), superoxide dismutase 1 (SOD1), superoxide dismutase 2 (SOD2) and peroxiredoxin 2 (PRX2). The assay was performed using Luminex xMAP technology (Merck Millipore) following manufacturer's instructions.

Insulin signaling analysis in response to 4-HNE treatment

The effect of 4-HNE treatment on the phosphorylation of IRS-1 (Ser636/Ser639), p70 S6 kinase (Thr389), GSK-3α/β (Ser21/Ser9) and p70 S6 kinase (Thr389) was quantified in human preadipocytes from IS and IR individuals. Briefly, preadipocytes were treated with 10µM of 4-HNE one day post-seeding for 15 days then lysed. Equal volumes of lysates were assayed using a commercial Bio-Plex Pro™ Cell Signaling Akt Panel following manufacturer's instructions.

Statistical analysis

Data are presented as mean±standard deviation (SD) for parametric data, median (interquartile range, IQ) for non-parameteric data in table 1 and mean±SEM in figures. Comparisons were performed with t-test, Wilcoxon–Mann–Whitney, 1-way ANOVA, or Linear regression model as appropriate using IBM SPSS statistics 21.

Results

General characteristics of study population

Eighteen obese and morbidly obese (BMI 43.2±5.09 kgm-2) young (30.4 ±8.3 years) females were recruited from amongst patients undergoing weight reduction surgery at HMC (Table 1). Participating subjects exhibited hypercholesterolaemia (4.8±0.96mM/L), hyperleptinemia (49.8±18.4 ng/ml) and hyperinsulinemia [11.4 (7.7-19.1) mIU/L] and were dichotomized into IS and IR groups based on their HOMA-IR index. Compared to age and BMI-matched IS subjects, IR individuals had higher levels of total cholesterol [4.3 (0.9) vs 5.2 (0.9), p=0.04] and ALT [20.1 (16-25) vs 32.4 (21.5-49), p=0.05] (Table 1).

Variables	Cohort (n=18)	IS (N=9)	IR (N=9)	*p* value
Age (year)	30.4 (8.3)	32 (10.7)	28.5 (4.5)	0.4
BMI (kg.m^{-2})	43.2 (5.09)	41.2 (1.9)	45.4 (6.6)	0.08
SBP (mmHg)	117.5 (39.35)	105.1 (40.3)	131.4 (35.4)	0.18
DBP (mmHg)	70.4 (10.9)	68.5 (9.2)	72.4 (12.8)	0.5
MAP	88.6 (13.45)	85.1 (8.3)	92.1 (17.03)	0.3
Cholesterol (mmol/L)	4.7 (0.96)	4.3 (0.9)	5.2 (0.9)	0.04
LDL (mmol/L)	3.2 (0.99)	2.8 (0.7)	3.6 (1.1)	0.09
Triglyceride (mmol/L)	1.1 (0.8-1.5)	0.9 (0.7-1.2)	1.4 (0.78-1.9)	0.12
Triglyceride/HDL	2.4 (1.4-3.4)	2.1 (1.2-2.3)	2.7 (1.2-2.3)	0.18
HDLC (mmol/L)	1.2 (0.2)	1.1 (0.3)	1.2 (0.2)	0.47
Leptin (ng/ml)	49.8 (18.4)	56.7 (19.1)	42.8 (15.5)	0.1
IL-6 (pg/ml)	3.2 (1.8)	2.8 (1.4)	3.6 (2.1)	0.32
FBG (mmol/L)	5.1 (0.6)	5.0 (0.6)	5.1 (0.6)	0.58
Insulin (mIU/L)	11.4 (7.7)	6.2 (2.9)	16.6 (7.5)	0.001
HOMA-IR	2.5 (1.7)	1.3 (0.6)	3.7 (1.5)	0.001
Albumin (g/L)	42.4 (5.6)	40.8 (4.9)	44.7 (6.7)	0.411
ALP (IU/L)	76.5 (61-92.5)	84.9 (65-104.5)	67 (48.2-78.5)	0.09
ALT (IU/L)	26.3 (17-33)	20.1 (16-25)	32.4 (21.5-49)	0.05
AST (IU/L)	20.1 (15.5-26.5)	17.4 (15-19)	23 (16-28.5)	0.07
Billirubin (µmol/L)	10.5 (4.8)	9.1 (3.7)	11.889 (5.5)	0.23

Table 1. General characteristics of participants. Obese and morbidly obese premenopausal female patients undergoing weight reduction surgery were dichotomized into two groups [insulin sensitive (IS) and insulin resistant (IR)] based on their homeostatic model assessment of insulin resistance (HOMA-IR) index. Components of metabolic syndrome were measured in IS and IR including BMI (body mass index), SBP (systolic blood pressure), DBP (diastolic blood pressure), MAP (mean arterial blood pressure), LDL (low density lipoprotein), HDL (high density lipoprotein), FPG (fasting plasma glucose), HOMA-IR, ALP (alkaline phosphatase), ALT (alanine transaminase), AST (aspartate aminotransferase). Data are presented as mean (SD) or median (IQR). Differences were tested by independent sample t test or Mann Whitney u test, $P<0.05$.

Characterization of 4-HNE staining in various cell types of the SC adipose tissue from obese patients

To confirm presence of 4-HNE stable adducts in adipose tissues, accumulation of 4-HNE in components of adipose tissues including adipocytes, connective tissues, blood vessels and inflammatory cells was analysed by immunohistochemistry (IHC) in all tested samples by 4-HNE antibody specific to Histidine epitope (data not shown). The strongest staining of 4-HNE stable adducts was detected in adipocytes and blood vessels; medium staining was in inflammatory cells and weakest staining was in connective tissues (Figure1). There were no significant differences in 4-HNE staining between IS and IR-adipose tissues confirming previous report [17].

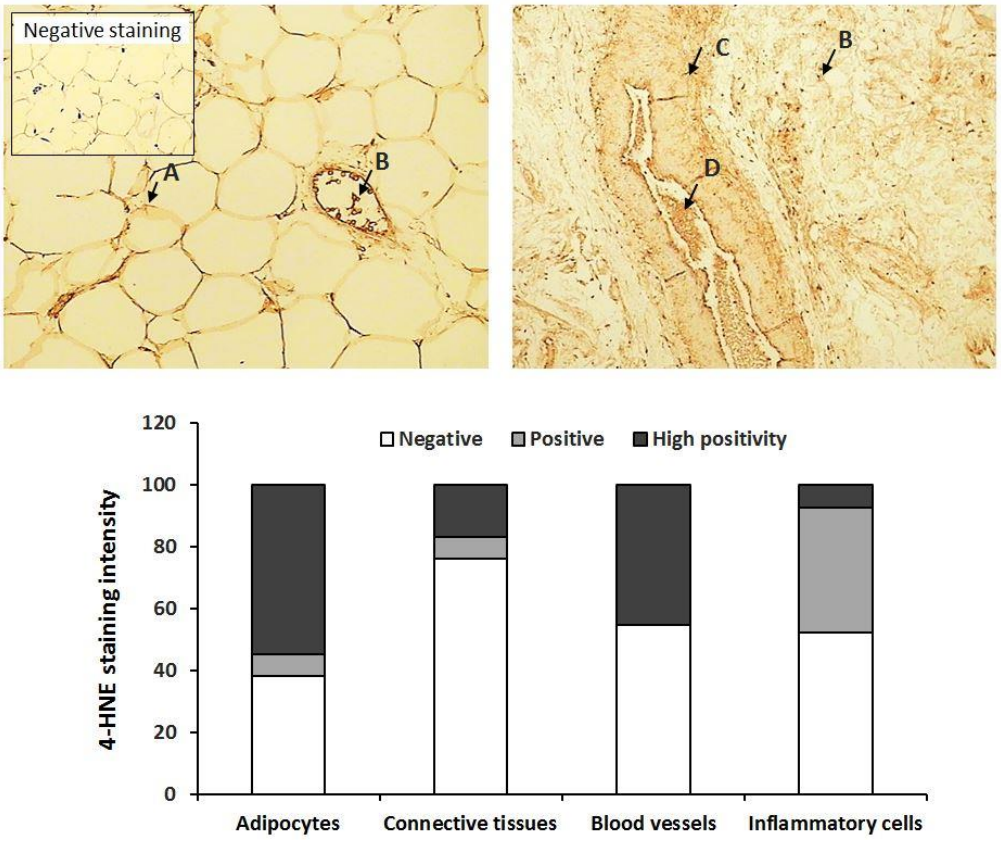

Figure1. 4-HNE IHC staining in SC adipose tissues from obese patients. Sections from ten adipose tissues were stained with for HNE-His and semi-quantified in adipocytes (A), inflammatory cells (B), connective tissues (C) and blood vessels (D) by an experienced pathologist without prior knowledge of the experimental groups.

Measurement of endogenous 4-HNE accumulation in proliferating and differentiating preadipocytes

The presence of 4-HNE adducts in paired cultures of proliferating preadipocytes and differentiated adipocytes was investigated. Detectable concentrations were quantified in both cultures with 30% increase in differentiated adipocytes compared to proliferating preadipocytes, possibly as a consequence of lipid accumulation with differentiation. IR differentiating preadipocytes exhibited 20% increase in 4-HNE accumulation than their IS counterparts (Figure 2).

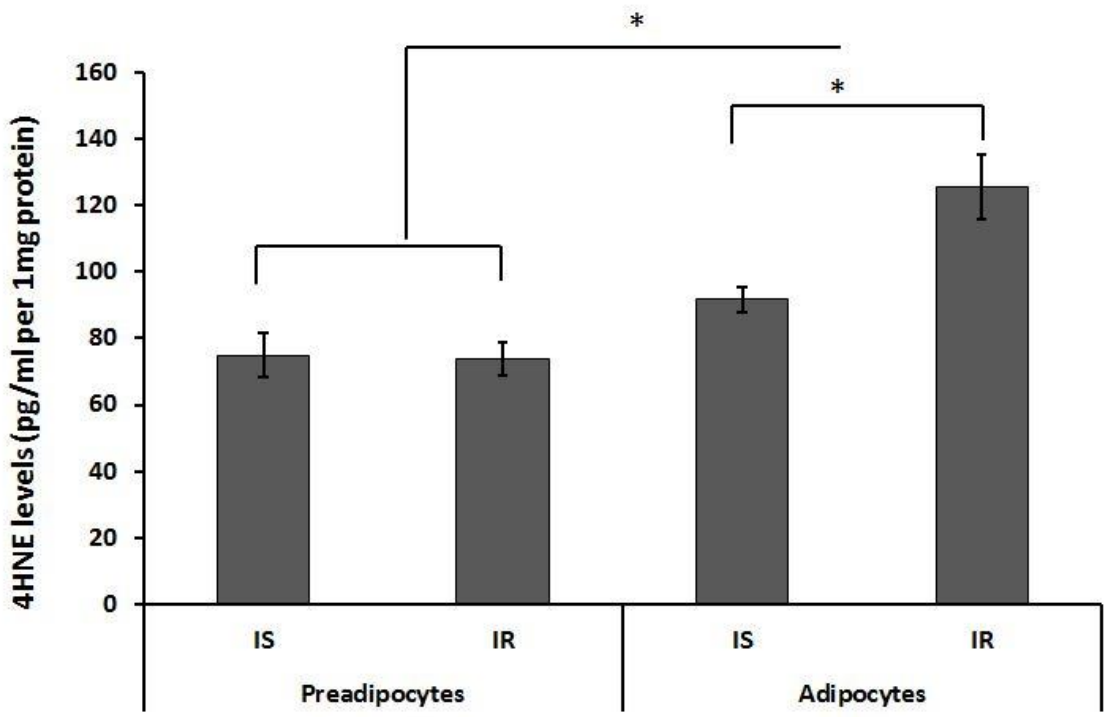

Figure 2. Endogenous 4-HNE accumulation in proliferating and differentiating preadipocytes. Levels of accumulated 4-HNE adducts were quantified in equal concentrations of protein lysates from paired cultures of proliferating preadipocytes and differentiated adipocytes from IS and IR individuals. Data are presented as Mean±SEM. N=15 (5 IS and 10 IR), *P<0.05, paired and independent sample t-test.

Preadipocyte proliferation, ROS generation and levels of ROS scavenging enzymes in response to 4-HNE treatment

The effect of exogenous 4-HNE treatment on preadipocytes growth and differentiation is shown in Figure 3. Treatment of preadipocytes with 4-HNE for 4 days exhibited a concentration-dependent inhibition of proliferation at a range of 2.5-20μM, compared to their untreated control, with higher concentrations causing cell death (Figure 3A). Acute treatment of preadipocytes with 10μM 4-HNE for 12 hours caused 2-4 folds elevated intracellular ROS and steady state hydrogen peroxide production compared to untreated cells ($p<0.05$, Figure 3B, C). It also increased levels of ROS scavenging enzymes including catalase, TRX1, PRX2, SOD1 and SOD2 (Figure 3D). Elevated levels of ROS scavenging enzymes were maintained following multiple exposures to 10μM of 4-HNE for 15 days, except for mitochondrial SOD2 activity (Figure 3E). When treated cells were dichotomized into IS and IR, there were no differences in levels of ROS scavenging

enzymes in response to short-term (Figure 3F) nor to long-term 4-HNE treatment except for catalase which exhibited a significantly higher elevation in IS differentiating preadipocytes compared to IR-derived counterparts (Figure 3G).

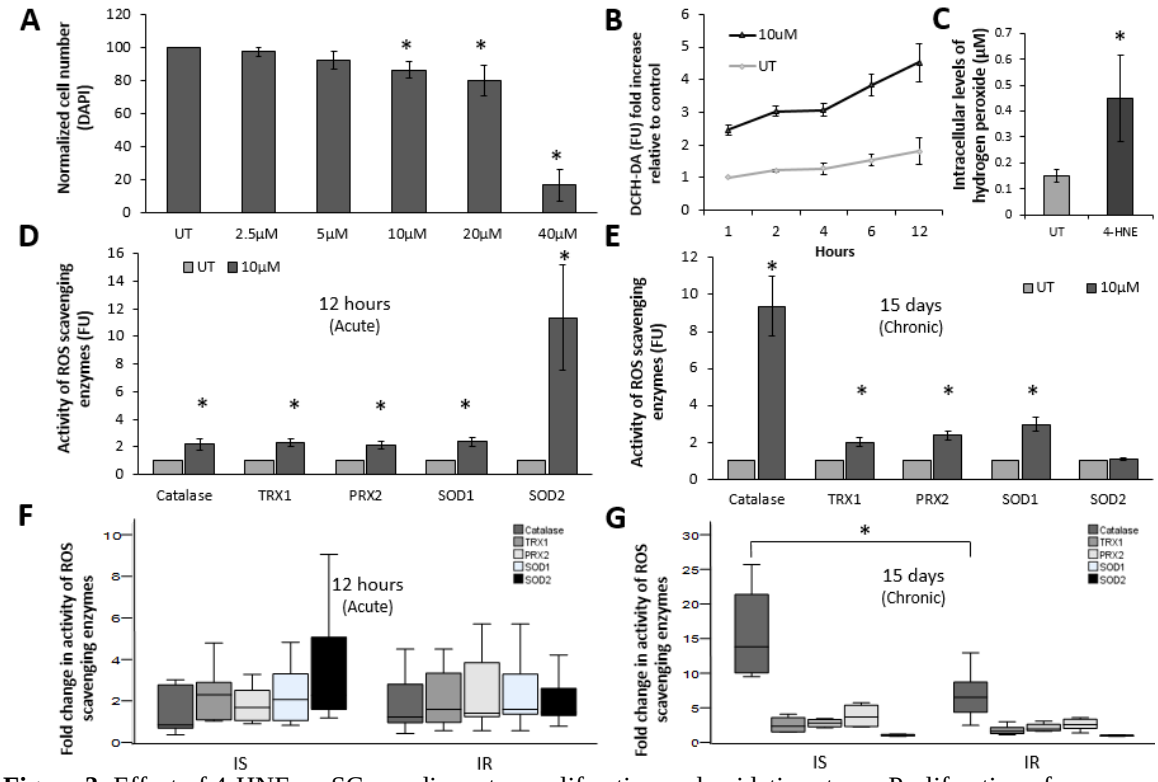

Figure 3. Effect of 4-HNE on SC preadipocytes proliferation and oxidative stress. Proliferation of preadipocytes upon acute exposure to different concentrations of 4-HNE was quantified by automated counting of cell number by DAPI staining (A). Reactive oxygen species (ROS) production was measured in response to 10 µM 4-HNE for up to 12 hours compared to untreated (UT) (B). Intracellular levels of hydrogen peroxide measured 12 hours upon 10 µM 4-HNE exposure compared to untreated (UT) (C). Levels of ROS scavenging enzymes (catalase, Trx1, Prx2, SOD1 and SOD2) in response to acute (12 hours, single exposure) (D) and Long-term (15 days, repeated exposures) treatment of preadipocytes to 10 µM 4-HNE (E). Comparison of levels of ROS scavenging enzymes between insulin sensitive (IS) and insulin resistant (IR)-derived preadipocytes in response to acute (F) and long-term exposures (G). Data are presented as Mean±SEM in A-E and as median (interquartile range) in F and G. N=18 (9 IS and 9 IR), *P<0.05, ANOVA and paired samples T-Test.

Growth and differentiation of IS vs IR preadipocytes in response to 4-HNE treatment

The effect of long-term treatment with 10μM of 4-HNE on preadipocyte growth and differentiation in IS and IR cells is presented in Figure 4. Exposure to multiple doses of 4-HNE led to reduction in growth and differentiation of preadipocytes in both groups (Figure 4A), marked by upregulation of anti-adipogenic FABP4 and down regulation of the adipogenic FASN and SREBF1 genes (Figure 4B). Whereas comparable levels of inhibition of cellular growth in response to 4-HNE were detected between IS and IR preadipocytes (Figure 4C), 4-HNE had a stronger inhibitory effect on IS-preadipocytes differentiation ($p<0.01$) compared to IR with a mean difference of 25.9% (IQR 3.9-55.7) (Figure 4D).

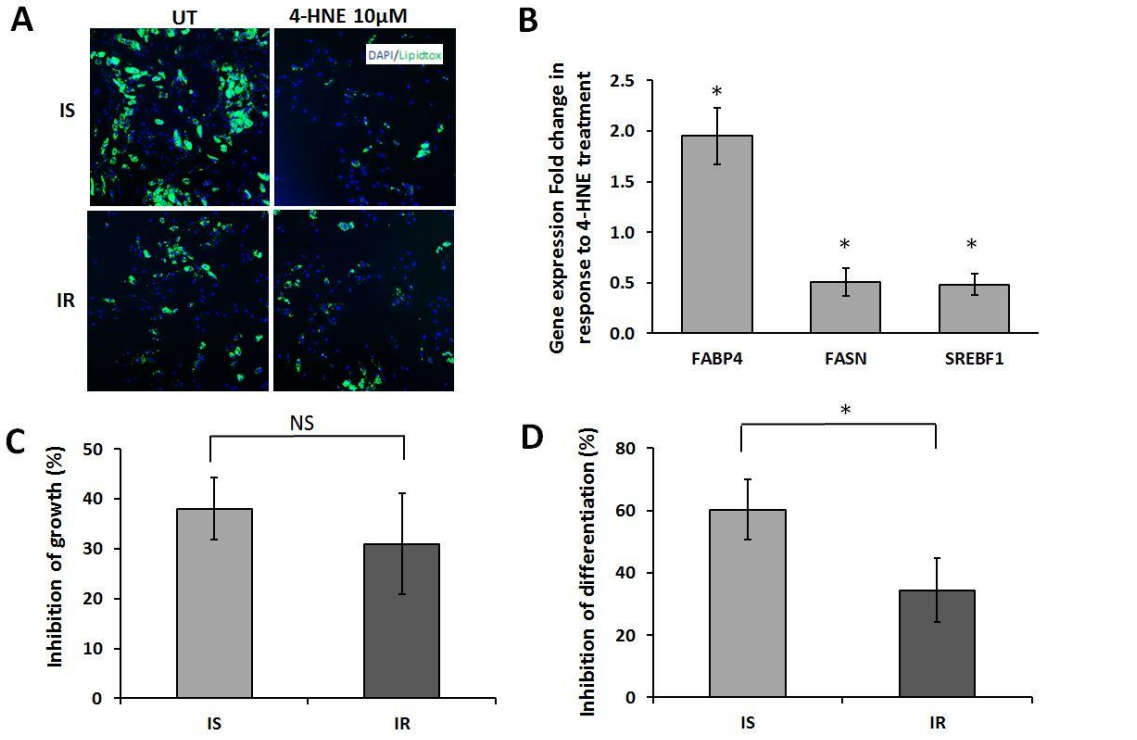

Figure 4. Effect of 4-HNE treatment on cellular growth and adipogenic capacity of preadipocytes derived from insulin sensitive and insulin resistant individuals. Total number of nuclei and number of differentiating preadipocytes from insulin sensitive (IS) and insulin resistant (IR) patients in response 10μM of 4-HNE was quantified by automated scoring of the number of nuclei (DAPI staining) and percentage of lipidtox positive cells to total number of cells (adipogenic capacity) by ArrayScan XTI Reader. Representative images of differentiated adipocytes with the selected fluorescently labelled lipid droplets are shown (A). FABP4, FASN and SREBF1 gene expression fold change in response to HNE treatment are shown (B). Percentages of inhibition of cellular growth (C) and adipogenic capacity (D)

compared to untreated controls were compared between IS and IR-derived cells. Data are presented as Mean±SEM. N=18 (9 per group).*P<0.05, Independent samples T-Test.

Analysis of insulin signaling in IS vs IR preadipocytes in response to 4-HNE treatment

Differences in insulin signaling pathway were detected between IS and IR preadipocytes in response to long-term treatment with 10μM of 4-HNE (Figure 5). IR-derived preadipocytes exhibited lower levels of phosphorylated IRS-1 and 70S6K at baseline compared to IS (Figure 5A and 5B), confirming their resistance to insulin action. Long-term treatment of preadipocytes from IS subjects to 10μM of 4-HNE caused significant dephosphorylation of IRS-1 (Figure 5A) and 70S6K (Figure 5B) and activation of GSK3α/β (Figure 5C) and BAD (Figure 5D), indicating development of IR phenotype. On the other hand, 4-HNE treatment of preadipocytes from IR subjects did not cause significant changes in the activation levels of IRS-1, 70S6K, GSK3α/β or BAD, suggesting their adaptation to 4-HNE action.

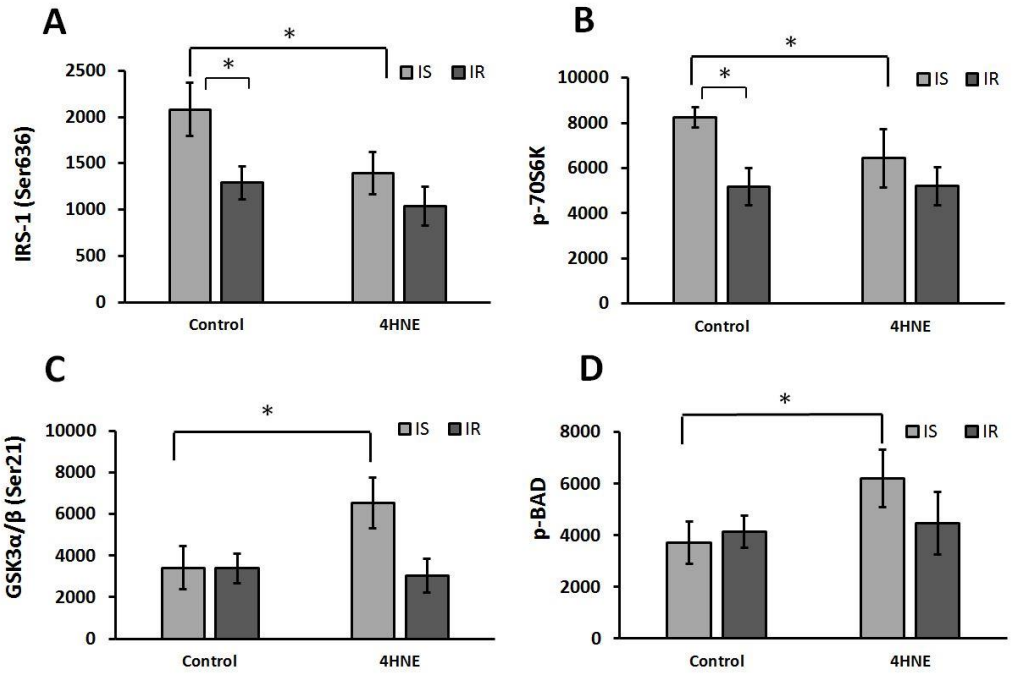

Figure 5. Effect of 4-HNE on insulin signaling in differentiating preadipocytes derived from insulin sensitive (IS) and insulin resistant (IR) individuals. Levels of phosphorylated IRS-1 (A), 70S6K (B), GSK3α/β (C) and BAD (D) were measured following long-term treatment of differentiating preadipocytes from IS and IR subjects to 10μM of 4-HNE. Data are presented as Mean±SEM. *P<0.05, Independent and paired samples T-Test. N=18 (9 per group).

Discussion

The lipid peroxidation product 4-HNE is one of the key mediators of oxidant-induced cell signaling and apoptosis [14], as it activates antioxidant defense systems at lower concentrations, while causes increased cell death with higher concentrations [38]. Therefore physiological levels of 4-HNE (up to 10 μM) in adipose tissues play a crucial role in redox homeostasis, whereas elevated 4-HNE levels (above 10 μM) can cause adipocyte dysfunction and insulin resistance [26, 39]. This study reports for the first time that long-term treatment of human primary preadipocytes from SC adipose tissues obtained from obese subjects with physiological concentrations of 4-HNE causes increased oxidative stress, inhibition of cell growth, loss of adipogenic capacity and induction of insulin resistance. The study also reports that preadipocytes from IS subjects are more prone to the effects of 4-HNE treatment than their IR counterpart. The heterogeneity in the sensitivity of SC preadipocytes to 4-HNE with regard to adipogenesis and insulin resistance in obese subjects may reflect the transient status of IS obesity that can change into a more adaptable IR phenotype over time.

Emerging data initially showed that elevated levels of 4-HNE in SC adipose tissues are located mainly within adipocytes and blood vessels in comparable levels between IS and IR subjects. Similar levels of 4-HNE between IS and IR adipose tissues, as reported previously [17], do not necessarily reflect a similar duration of exposure to 4-HNE as it may merely represent a snapshot of a long processes that preceded the onset of obesity. Indeed, this report shows that spontaneously accumulated levels of 4-HNE adducts are higher in cultured differentiating IR-preadipocytes compared to a similar age IS cultures, perhaps as a result of increased ROS production in IR preadipocytes as we reported previously [7]. This data indeed confirms an important biological role for 4-HNE by showing its spontaneous accumulation in differentiating preadipocytes that alters cellular redox homeostasis.

The data indicated that acute 4-HNE treatment of preadipocytes at a concentration that is at the lower end of the pathophysiological range [15], and reported previously in 3T3L-1 preadipocytes [26], increases intracellular hydrogen peroxide as well as ROS production in preadipocytes in a concentration-dependent manner, which is also associated with increased levels of ROS scavenging enzymes including catalase, PRX2, TRX1, SOD1 and SOD2. Acute exposure to 4-HNE had the most pronounced effect on SOD2, suggesting that mitochondria are important early targets for 4-HNE induced redox imbalance in preadipocytes. However, long-term exposure to 4-HNE highlighted the role of catalase, but not SOD2, as the main anti-oxidant defense mechanism in differentiating preadipocytes against oxidative stress mediated by repeated 4-HNE exposure (Figure 3). This could be one of the mechanisms triggered to enable cellular adaptation to 4-HNE-induced intracellular H_2O_2 production [40]. Moreover, elevated catalase could also suggest changes in the lipid metabolism as it is an important enzyme in decomposing H_2O_2 produced during beta oxidation of fatty acids by flavin adenine dinucleotide (FAD)-oxidases [41]. The increased catalase activity in 4-HNE treated differentiating preadipocytes was more significant in IS-derived cells, suggesting higher sensitivity to 4-HNE-induced oxidative stress, compared to IR-derived counterparts. Taken together, our data confirm both earlier *in vitro* findings of increased ROS production in response to 4-HNE in 3T3L-1 preadipocyte cell line [26] and *in vivo* observations of elevated ROS scavenging enzymes in adipose tissues from obese subjects with increased 4-HNE levels [17], adding to the significant role 4-HNE plays in modulating adipose tissue homeostasis.

Long-term treatment of SC preadipocytes with a physiological concentration of 4-HNE lowered adipogenesis in preadipocytes obtained from both IS and IR individuals, with a greater inhibition in IS-derived preadipocytes (Figure 4). The important role of 4-HNE in adipogenesis is further supported by gene expression studies of transcriptional regulation of adipocyte differentiation pathway. Key adipogenic genes including pro-adipogenic genes SREBF1 [42, 43] and FASN [44] were down regulated and anti-adipogenic gene FABP4 [45] known to play a role in fatty acid uptake, transport and metabolism was upregulated [46]. The lower susceptibility of IR preadipocytes to 4-HNE damaging effect

may suggest that IR preadipocytes have reached a certain degree of adaptation to oxidative stress damage as they developed resistance to insulin. Indeed we have observed that, in response to elevated 4-HNE, IR preadipocytes have higher expression of FABP4 compared to IS preadipocytes (data not shown). In addition to its anti-adipogenic role, FABP4 is a known cellular target [47] and a scavenger of 4-HNE [48]. The IS preadipocytes, on the other hand, were still sensitive to the damaging effect of 4-HNE-induced oxidative stress that may eventually lead to metabolic complications associated with insulin resistance and development of T2DM.

As impaired adipogenesis and subsequent ectopic lipid accumulation are associated with insulin resistance [49], the greater sensitivity of IS preadipocytes to 4-HNE could also cause impaired glucose homeostasis. Indeed, our data indicated that long-term treatment of IS preadipocytes with a physiological concentration of 4-HNE triggered their resistance to insulin by deactivating the insulin signaling components IRS1 and p70S6K and activating GSK3α/β and BAD that are under the negative control of Akt [50]. As expected, IR-preadipocytes showed no change in their insulin signaling in response to 4-HNE treatment as they are already resistant to its actions as seen at baseline. Although previous reports have shown that 4-HNE can induce insulin resistance in skeletal muscle cells [39], this is the first report of induction of insulin resistance in human SC differentiating preadipocytes in response to 4-HNE. Taken together, Figure 6 depicts proposed actions for 4-HNE in differentiating preadipocytes. Previous studies have shown that abolishing 4-HNE-induced oxidative stress in 3T3L1 by pharmacological intervention leads to lowering inflammation-related cyclooxygenase expression [23], reversal of 4-HNE deleterious effects and improvement in insulin sensitivity [51]. Future work will focus on pharmacological intervention aimed at alleviating insulin resistance and oxidative stress in IR preadipocytes.

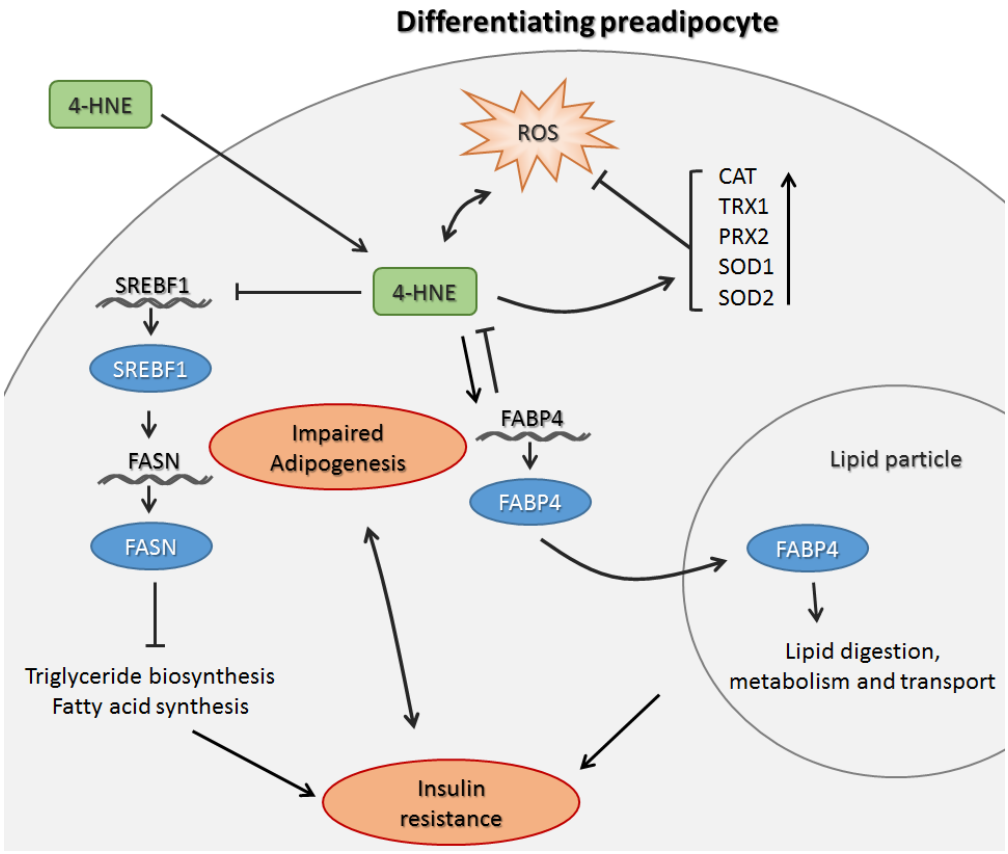

Figure6. A scheme representing 4-HNE actions in adipocytes, highlighting effects on ROS production, modulation of lipid metabolism, impairment of adipogenesis and development of insulin resistance.

Conclusions

In conclusion, this study provides novel evidence for 4-HNE-mediated inhibition of human preadipocytes growth, impairment of adipogenesis and induction of insulin resistance, thus highlighting its crucial role in the progression obesity-associated metabolic syndrome. The data also identifies 4-HNE as a key player in the pathophysiology of adipose tissue in IS obesity and potentially a therapeutic target before progression into IR obesity.

Acknowledgements

This work was supported by Qatar National Research Fund [QNRF grant number NPRP6-235-1-048] for MAE, MJ and WK. We would also like to thank Dr. Vidya Mohamed Ali for the critical review of the manuscript.

Contribution statement

MAE designed experiments, supervised progress, analyzed data and wrote the article. SM carried out most of data acquisition and analysis and helped with drafting article. WK advised on experimental design, supervised SM progress and provided expertise in stem cell biology. AM & FK helped with experimental work and data analysis. MB provided samples and information of subjects who participated in this study. KZ and NZ performed immunohistochemistry and analyzed data. GW generated and produced 4-HNE antibodies. MA advised on experimental design. MJ conceived the study, designed the experiments, supervised progress, analyzed data and wrote the article. All authors have provided critical revision of the draft manuscript and have approved the final version.

References

[1] C. Bogardus, S. Lillioja, D.M. Mott, C. Hollenbeck, G. Reaven, Relationship between degree of obesity and in vivo insulin action in man, Am J Physiol 248(3 Pt 1) (1985) E286-91.

[2] D. Samocha-Bonet, D.J. Chisholm, K. Tonks, L.V. Campbell, J.R. Greenfield, Insulin-sensitive obesity in humans - a 'favorable fat' phenotype?, Trends Endocrinol Metab 23(3) (2012) 116-24.

[3] M. Bluher, Are metabolically healthy obese individuals really healthy?, Eur J Endocrinol 171(6) (2014) R209-19.

[4] K.L. Spalding, E. Arner, P.O. Westermark, S. Bernard, B.A. Buchholz, O. Bergmann, L. Blomqvist, J. Hoffstedt, E. Naslund, T. Britton, H. Concha, M. Hassan, M. Ryden, J. Frisen, P. Arner, Dynamics of fat cell turnover in humans, Nature 453(7196) (2008) 783-7.

[5] P. Isakson, A. Hammarstedt, B. Gustafson, U. Smith, Impaired preadipocyte differentiation in human abdominal obesity: role of Wnt, tumor necrosis factor-alpha, and inflammation, Diabetes 58(7) (2009) 1550-7.

[6] L.B. Salans, J.L. Knittle, J. Hirsch, The role of adipose cell size and adipose tissue insulin sensitivity in the carbohydrate intolerance of human obesity, J Clin Invest 47(1) (1968) 153-65.

[7] S. Almuraikhy, W. Kafienah, M. Bashah, I. Diboun, M. Jaganjac, F. Al-Khelaifi, H. Abdesselem, N.A. Mazloum, M. Alsayrafi, V. Mohamed-Ali, M.A. Elrayess, Interleukin-

6 induces impairment in human subcutaneous adipogenesis in obesity-associated insulin resistance, Diabetologia (2016).

[8] T. Tchkonia, D.E. Morbeck, T. Von Zglinicki, J. Van Deursen, J. Lustgarten, H. Scrable, S. Khosla, M.D. Jensen, J.L. Kirkland, Fat tissue, aging, and cellular senescence, Aging Cell 9(5) (2010) 667-84.

[9] K.F. Petersen, G.I. Shulman, Etiology of insulin resistance, Am J Med 119(5 Suppl 1) (2006) S10-6.

[10] S. Furukawa, T. Fujita, M. Shimabukuro, M. Iwaki, Y. Yamada, Y. Nakajima, O. Nakayama, M. Makishima, M. Matsuda, I. Shimomura, Increased oxidative stress in obesity and its impact on metabolic syndrome, J Clin Invest 114(12) (2004) 1752-61.

[11] F. Gueraud, M. Atalay, N. Bresgen, A. Cipak, P.M. Eckl, L. Huc, I. Jouanin, W. Siems, K. Uchida, Chemistry and biochemistry of lipid peroxidation products, Free Radic Res 44(10) (2010) 1098-124.

[12] A. Higdon, A.R. Diers, J.Y. Oh, A. Landar, V.M. Darley-Usmar, Cell signalling by reactive lipid species: new concepts and molecular mechanisms, Biochem J 442(3) (2012) 453-64.

[13] M. Jaganjac, O. Tirosh, G. Cohen, S. Sasson, N. Zarkovic, Reactive aldehydes--second messengers of free radicals in diabetes mellitus, Free Radic Res 47 Suppl 1 (2013) 39-48.

[14] G. Bauer, N. Zarkovic, Revealing mechanisms of selective, concentration-dependent potentials of 4-hydroxy-2-nonenal to induce apoptosis in cancer cells through inactivation of membrane-associated catalase, Free Radic Biol Med 81 (2015) 128-44.

[15] Z.H. Chen, E. Niki, 4-hydroxynonenal (4-HNE) has been widely accepted as an inducer of oxidative stress. Is this the whole truth about it or can 4-HNE also exert protective effects?, IUBMB Life 58(5-6) (2006) 372-3.

[16] S. Dalleau, M. Baradat, F. Gueraud, L. Huc, Cell death and diseases related to oxidative stress: 4-hydroxynonenal (HNE) in the balance, Cell Death Differ 20(12) (2013) 1615-30.

[17] A. Jankovic, A. Korac, B. Srdic-Galic, B. Buzadzic, V. Otasevic, A. Stancic, M. Vucetic, M. Markelic, K. Velickovic, I. Golic, B. Korac, Differences in the redox status of human visceral and subcutaneous adipose tissues--relationships to obesity and metabolic risk, Metabolism 63(5) (2014) 661-71.

[18] M. Vazdar, P. Jurkiewicz, M. Hof, P. Jungwirth, L. Cwiklik, Behavior of 4-hydroxynonenal in phospholipid membranes, J Phys Chem B 116(22) (2012) 6411-5.

[19] N. Zarkovic, A. Cipak, M. Jaganjac, S. Borovic, K. Zarkovic, Pathophysiological relevance of aldehydic protein modifications, J Proteomics 92 (2013) 239-47.

[20] G. Poli, R.J. Schaur, W.G. Siems, G. Leonarduzzi, 4-hydroxynonenal: a membrane lipid oxidation product of medicinal interest, Med Res Rev 28(4) (2008) 569-631.

[21] M. Parola, G. Bellomo, G. Robino, G. Barrera, M.U. Dianzani, 4-Hydroxynonenal as a biological signal: molecular basis and pathophysiological implications, Antioxid Redox Signal 1(3) (1999) 255-84.

[22] G. Cohen, Y. Riahi, S. Sasson, Lipid peroxidation of poly-unsaturated fatty acids in normal and obese adipose tissues, Arch Physiol Biochem 117(3) (2011) 131-9.

[23] B. Zarrouki, A.F. Soares, M. Guichardant, M. Lagarde, A. Geloen, The lipid peroxidation end-product 4-HNE induces COX-2 expression through p38MAPK activation in 3T3-L1 adipose cell, FEBS Lett 581(13) (2007) 2394-400.

[24] S. Le Lay, G. Simard, M.C. Martinez, R. Andriantsitohaina, Oxidative stress and metabolic pathologies: from an adipocentric point of view, Oxid Med Cell Longev 2014 (2014) 908539.

[25] X. Zhang, Z. Wang, J. Li, D. Gu, S. Li, C. Shen, Z. Song, Increased 4-hydroxynonenal formation contributes to obesity-related lipolytic activation in adipocytes, PLoS One 8(8) (2013) e70663.

[26] K. Dasuri, P. Ebenezer, S.O. Fernandez-Kim, L. Zhang, Z. Gao, A.J. Bruce-Keller, L.R. Freeman, J.N. Keller, Role of physiological levels of 4-hydroxynonenal on adipocyte biology: implications for obesity and metabolic syndrome, Free Radic Res 47(1) (2013) 8-19.

[27] V.R. Mali, M. Deshpande, G. Pan, R.A. Thandavarayan, S.S. Palaniyandi, Impaired ALDH2 activity decreases the mitochondrial respiration in H9C2 cardiomyocytes, Cell Signal 28(2) (2016) 1-6.

[28] S.M. Grundy, H.B. Brewer, Jr., J.I. Cleeman, S.C. Smith, Jr., C. Lenfant, A. American Heart, L. National Heart, I. Blood, Definition of metabolic syndrome: Report of the National Heart, Lung, and Blood Institute/American Heart Association conference on scientific issues related to definition, Circulation 109(3) (2004) 433-8.

[29] G. Waeg, G. Dimsity, H. Esterbauer, Monoclonal antibodies for detection of 4-hydroxynonenal modified proteins, Free Radic Res 25(2) (1996) 149-59.

[30] Z.K. Zivkovic Morana, Skrinjar Ljubomir, Georg Waeg, Poljak-Blazi Marija, Borovic Suzana, Schaur Rudolf Jörg, Zarkovic Neven A new method for detection of HNE-histidine conjugates in rat inflammatory cells. , Croatica Chemica Acta 78 (2005) 91-98.

[31] M. Jaganjac, M. Poljak-Blazi, R.J. Schaur, K. Zarkovic, S. Borovic, A. Cipak, M. Cindric, K. Uchida, G. Waeg, N. Zarkovic, Elevated neutrophil elastase and acrolein-protein adducts are associated with W256 regression, Clin Exp Immunol 170(2) (2012) 178-85.

[32] K. Zarkovic, K. Uchida, D. Kolenc, L. Hlupic, N. Zarkovic, Tissue distribution of lipid peroxidation product acrolein in human colon carcinogenesis, Free Radic Res 40(6) (2006) 543-52.

[33] C.M. Spickett, I. Wiswedel, W. Siems, K. Zarkovic, N. Zarkovic, Advances in methods for the determination of biologically relevant lipid peroxidation products, Free Radic Res 44(10) (2010) 1172-202.

[34] B.A. Bunnell, B.T. Estes, F. Guilak, J.M. Gimble, Differentiation of adipose stem cells, Methods Mol Biol 456 (2008) 155-71.

[35] M.J. Lee, Y. Wu, S.K. Fried, A modified protocol to maximize differentiation of human preadipocytes and improve metabolic phenotypes, Obesity (Silver Spring) 20(12) (2012) 2334-40.

[36] M. Poljak-Blazi, M. Jaganjac, I. Sabol, B. Mihaljevic, M. Matovina, M. Grce, Effect of ferric ions on reactive oxygen species formation, cervical cancer cell lines growth and E6/E7 oncogene expression, Toxicol In Vitro 25(1) (2011) 160-6.

[37] B.A. Wagner, J.R. Witmer, T.J. van 't Erve, G.R. Buettner, An Assay for the Rate of Removal of Extracellular Hydrogen Peroxide by Cells, Redox Biol 1(1) (2013) 210-217.

[38] Y.C. Awasthi, Y. Yang, N.K. Tiwari, B. Patrick, A. Sharma, J. Li, S. Awasthi, Regulation of 4-hydroxynonenal-mediated signaling by glutathione S-transferases, Free Radic Biol Med 37(5) (2004) 607-19.

[39] N.J. Pillon, M.L. Croze, R.E. Vella, L. Soulere, M. Lagarde, C.O. Soulage, The lipid peroxidation by-product 4-hydroxy-2-nonenal (4-HNE) induces insulin resistance in skeletal muscle through both carbonyl and oxidative stress, Endocrinology 153(5) (2012) 2099-111.

[40] A. Cipak, M. Jaganjac, O. Tehlivets, S.D. Kohlwein, N. Zarkovic, Adaptation to oxidative stress induced by polyunsaturated fatty acids in yeast, Biochim Biophys Acta 1781(6-7) (2008) 283-7.

[41] H.R. Waterham, S. Ferdinandusse, R.J. Wanders, Human disorders of peroxisome metabolism and biogenesis, Biochim Biophys Acta 1863(5) (2016) 922-33.

[42] L. Fajas, K. Schoonjans, L. Gelman, J.B. Kim, J. Najib, G. Martin, J.C. Fruchart, M. Briggs, B.M. Spiegelman, J. Auwerx, Regulation of peroxisome proliferator-activated receptor gamma expression by adipocyte differentiation and determination factor 1/sterol regulatory element binding protein 1: implications for adipocyte differentiation and metabolism, Mol Cell Biol 19(8) (1999) 5495-503.

[43] J.T. Ayala-Sumuano, C. Velez-Delvalle, A. Beltran-Langarica, M. Marsch-Moreno, J. Cerbon-Solorzano, W. Kuri-Harcuch, Srebf1a is a key regulator of transcriptional control for adipogenesis, Sci Rep 1 (2011) 178.

[44] L.H. Liu, X.K. Wang, Y.D. Hu, J.L. Kang, L.L. Wang, S. Li, Effects of a fatty acid synthase inhibitor on adipocyte differentiation of mouse 3T3-L1 cells, Acta Pharmacol Sin 25(8) (2004) 1052-7.

[45] T. Garin-Shkolnik, A. Rudich, G.S. Hotamisligil, M. Rubinstein, FABP4 attenuates PPARgamma and adipogenesis and is inversely correlated with PPARgamma in adipose tissues, Diabetes 63(3) (2014) 900-11.

[46] A.W. Zimmerman, J.H. Veerkamp, New insights into the structure and function of fatty acid-binding proteins, Cell Mol Life Sci 59(7) (2002) 1096-116.

[47] P.A. Grimsrud, M.J. Picklo, Sr., T.J. Griffin, D.A. Bernlohr, Carbonylation of adipose proteins in obesity and insulin resistance: identification of adipocyte fatty acid-binding protein as a cellular target of 4-hydroxynonenal, Mol Cell Proteomics 6(4) (2007) 624-37.

[48] A. Bennaars-Eiden, L. Higgins, A.V. Hertzel, R.J. Kapphahn, D.A. Ferrington, D.A. Bernlohr, Covalent modification of epithelial fatty acid-binding protein by 4-hydroxynonenal in vitro and in vivo. Evidence for a role in antioxidant biology, J Biol Chem 277(52) (2002) 50693-702.

[49] H.M. Findeisen, K.J. Pearson, F. Gizard, Y. Zhao, H. Qing, K.L. Jones, D. Cohn, E.B. Heywood, R. de Cabo, D. Bruemmer, Oxidative stress accumulates in adipose tissue during aging and inhibits adipogenesis, PLoS One 6(4) (2011) e18532.

[50] B.D. Manning, L.C. Cantley, AKT/PKB signaling: navigating downstream, Cell 129(7) (2007) 1261-74.

[51] D. Demozay, J.C. Mas, S. Rocchi, E. Van Obberghen, FALDH reverses the deleterious action of oxidative stress induced by lipid peroxidation product 4-

hydroxynonenal on insulin signaling in 3T3-L1 adipocytes, Diabetes 57(5) (2008) 1216-26.